Functional Stability of a Ferromagnetic Polycrystalline Ni_2MnGa High Temperature Shape Memory Alloy

M.A. Azeem[a,b,c,*], N.G. Jones[a,d], S.L. Raghunathan[a,e], V.A. Vorontsov[a], D. Dye[a,*]

[a] *Dept. Materials, Royal School of Mines, Imperial College, Prince Consort Road, South Kensington, London SW7 2BP, UK*
[b] *School of Materials, The University of Manchester, Manchester M13 9PL, UK*
[c] *Research Complex at Harwell, Harwell Science & Innovation Campus, Didcot OX11 0FA, UK*
[d] *Department of Materials Science and Metallurgy, University of Cambridge, 27 Charles Babbage Road, Cambridge, CB3 0FS, UK*
[e] *Cryogenic Ltd, Unit 6, Acton Park Estate, The Vale, Acton, London W3 7QE*

Abstract

Electrocaloric Ni_2MnGa is of interest for solid state refrigeration applications, as well as a high temperature thermal shape memory alloy. Here, polycrystalline $Ni_{54}Mn_{25}Ga_{21}$ is examined using in situ synchrotron X-ray diffraction. The initial martensite (M_f) and austenite (A_f) finish temperatures were found to be 232 °C and 298 °C respectively. M_f was observed to decline by 8 °C/cycle and A_f increased by 1 °C/cycle. Both below and surprisingly, above the Curie temperature, the application of an e.m.f. was found to affect the lattice parameters measured. A change in the thermal expansion of the two phases was found around the Curie temperature.

Keywords: Ferromagnetic shape memory alloy; synchrotron radiation; thermal expansion; intermetallic compounds

Ferromagnetic shape memory alloys (fSMAs) based on the Ni-Mn-Ga system [1] are of great interest both as actuators and as magnetocaloric materials. Examples range from fast actuation (using an applied magnetic field) in aerodynamic control surfaces [2, 3] to magnetically operated solid-state heat pumps offering coefficients of performance (COP) > 4 [4]. There has also been interest in using the mechanically induced phase transformation in conventional SMAs (*e.g.* NiTi) in a similar way [5, 6]. Large magnetic field induced strains (MFIS) are widely reported in these alloys [7–11] and the underlying mechanism is thought to be the magnetically induced mobility of twin interfaces [8, 12].

Shape memory functionality was first observed in the Hesuler compound Ni_2MnGa [13] and the ferromagnetic phase transformation was discovered almost a decade later in off-stoichiometric Ni-Mn-Ga alloys [14]. The martensite transformation temperatures (T_m) are sensitive to deviations in stoichiometry; Ni substitution for Ga result in changes of ~50 K per at.% [1, 15, 16], but this results in only a modest change in the Curie temperature (T_c) [1, 15]. It is observed that the T_m increases linearly with the alloy electron concentration, *i.e.,* increases in the electron per atom ratio (e/a)[16–18]. Therefore, in developing high temperature Ni-Mn-Ga alloys, replacement of Ga by Ni are generally preferred as Ni has the greatest number of valence electrons and since the Ni fraction is greatest. For example, the M_f in a $Ni_{54}Mn_{24.7}Ga_{21.3}$ alloy (e/a = 7.768) [15] is ~215 K higher than in near-stochiometric $Ni_{50}Mn_{25}Ga_{25}$ (e/a = 7.5) [7, 18–20].

Irrespective of composition, the austenite in Ni-Mn-Ga alloys is reported to be $Fm\bar{3}m$ but the martensite crystal structure varies with small changes in composition [15, 21]. Both modulated and non-modulated martensites have been reported; 5M and 7M martensites are observed in alloys with Curie temperatures (T_c) higher than T_m whilst non-modulated martensites are observed in alloys where $T_c < T_m$ [15]. In Mn-rich alloys with ~20 at.% Ga, orthrhombic and tetragonal martensites are observed, and for certain compositions both forms can co-exist [21]. In the tetragonal martensite increases in e/a increases the tetragonality, c_t/a_t [19].

Single crystals have been used in most investigations of Ni-Mn-Ga alloys, but single crystal fabrication will limit the range of product forms that can be economically produced, so polycrystalline Ni-Mn-Ga alloys are highly desirable. In this context, purely thermal high temperature Ni_2MnGa actuators are also of interest, as conventional NiTi-based SMAs are limited to austenite finish temperatures of ~90°C. Normally, SMAs show significant functional fatigue, with the transformation temperatures dropping with each cycle, and so practical actuators with service lives of thousands of cycles remain difficult to produce.

Here, we focus on the characterisation of the thermal transformation in polycrystalline off-stoichiometry $Ni_{54}Mn_{25}Ga_{21}$ by synchrotron X-ray diffraction, with an emphasis on the evolution of the unit cell parameters of the phases. This particular composition was chosen to satisfy the requirement that the transformation be single step (cubic↔tetragonal) [22, 23] and to obtain a high temperature shape memory candidate with T_m in excess of 200°C [22].

The alloy was prepared by vacuum arc melting pure elemental Ni, Mn and Ga in pure argon. The ingot was remelted four

*Corresponding author
Email address: mohammed.azeem@manchester.ac.uk, david.dye@imperial.ac.uk (D. Dye)

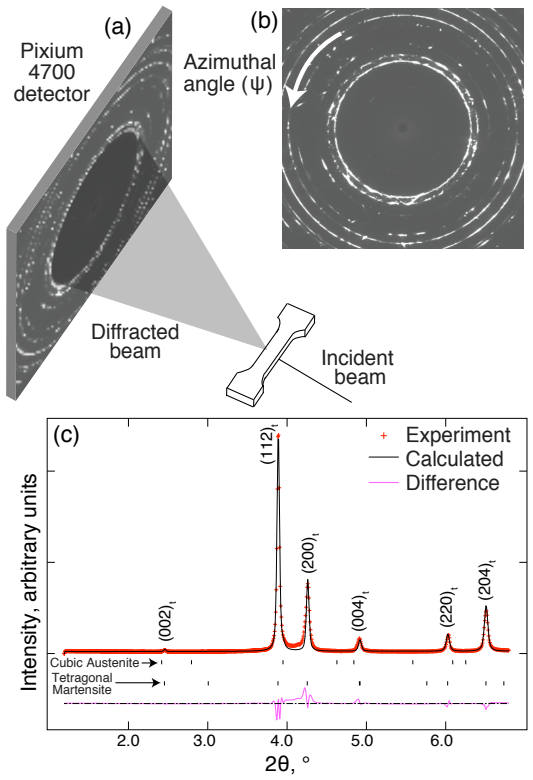

Figure 1: (a) Schematic of the synchrotron X-ray diffraction setup, (b) Complete Debye-Scherrer rings from tetragonal martensite and (c) Diffraction spectra after 360° intensity integration across diffraction rings in (b)

times and inter-melt flipped to minimise elemental segregation. The ≈60 g ingot was encapsulated in a quartz tube and then homogenised at 900°C for 24 h. The ingot was then packed in Ti powder in a mild steel can and 80% hot rolled at 900°C. $0.5 \times 0.5 \times 30$ mm gauge length specimens were then fabricated by grinding and electro-discharge machining. Differential scanning calorimetry using a Mettler Toledo DSC 822^e instrument was used to obtain initial estimates of the transformation temperatures. The composition was also checked at this stage by SEM-EDX and found to be within the measurement error (∼ 0.5 at.%) of the target composition. Light element pickup such as O was therefore not determined. The specimen was then thermally cycled at a rate of 2 °Cs^{-1} at zero load in an Instron5 kN resistance heating electro-thermal mechanical testing machine (ETMT) at the ID15B powder diffraction beamline at the ESRF, Grenoble France, Figure 1. The sample temperature was measured by using R-type thermocouple mounted on the sample surface, within 0.1 mm of the scanned volume. A wavelength of 0.1427 Å was used and the incident beam was approx. 0.5×0.5 mm in size, giving a sampled volume of $0.5 \times 0.5 \times 0.5 = 0.125$ mm^3. A Thales Pixium 4700 detector [24] was used to collect complete Debeye-Scherrer diffraction rings (Figure 1b) at a sample-detector distance of 1.228 m. A LaB_6 calibration powder was used to determine the instrument parameters. Phase fractions and lattice parameters were evaluated using the generalized structural analysis package (GSAS) [26, 27] and the area detector analysis package Fit2D [28]. Whole-ring integrations were used; the analysis was not found to be sensitive to orientation around the ring; *i.e* there were no effects induced by, *e.g.* the rolling texture. This issue has been examined in our previous work [29, 30].

The high temperature (austenite) phase in $Ni_{54}Mn_{25}Ga_{21}$ has an F m $\bar{3}$ m crystal structure with Ni at (1/4, 1/4, 1/4), Mn at (1/2,1/2,1/2) and Ga at (0,0,0) and $a_c = 5.8468 \pm 0.0003$ at 320 °C. For thermal cycling in the absence of stress and magnetic field, the martensite is tetragonal. The room temperature lattice parameters of the martensite were found to be $a_t = 3.8391 \pm 0.0003$, $c_t = 6.650 \pm 0.001$ and $c_t/a_t = 1.732$. Comparing these with the lattice parameters for $Ni_{53}Mn_{25}Ga_{22}$ reported by Cong *et. al.* [23] of $a_t = 3.865$, $c_t = 6.596$ and $c_t/a_t = 1.707$, the increase in e/a achieved by increasing Ni (at the expense of Ga) in the current alloy appears to change the c/a ratio considerably. The main orientation relationship in $Ni_{53}Mn_{25}Ga_{22}$ is reported to be $(111)_c \| (101))_t$, $[110])_c \| [111])_t$ [1, 31].

The transformation sequence in the first thermal cycle is shown in Figure 2. A large dilation in the $d_{(200)}$ interplanar spacing in the tetragonal martensite was clearly visible on heating and cooling. A new peak emerged in vicinity of the tetragonal (200) peak during the initial stages of cooling, but apart from this no additional peaks were observed elsewhere in the spectra. Therefore it is difficult to confirm the existence of an intermediate martensite phase. A subtle yet visible shift in the (200) tetragonal peak is observed (arrowed) on final cooling and before reheating began.

The Rietveld-refined lattice parameters and phase fractions are shown in Figure 3. The transformation from tetragonal to cubic begins on heating at around 213°C with 80% of the cubic phase appearing over a temperature range of 227 − 258 °C, after which the transformation rate decreases with temperature before final completion at 286°C. The measurement points occur approximately every 5 °C, allowing the austenite and martensite start and finish temperatures (at 90% / 10% phase fraction) to be interpolated with an accuracy of around 3°C, Table 1. The fitted lattice parameters, Figure 3, show almost no shift between successive thermal cycles, which is a good indicator of thermal stability. For example, the change in a_t at 125 °C after four thermal cycles was only 0.04% (Table 1). On initial heating, a_t increased at a rate of $\approx 77 \times 10^{-6}$ °C^{-1} and c_t decreases with a thermal expansion coefficient of -69×10^{-6} °C^{-1}. At ≈160°C (near the Curie temperature estimated elsewhere [15, 23]), a visible change in linearity is observed and the thermal expansion / contraction appears to accelerate; *i.e.,* a_t then dilates and c_t constricts at a more rapidly than before. These events are schematically highlighted in the final subfigure in Figure 3. The reverse behaviour is observed on cooling and again the inflection point is ≈160 °C. One can speculate that this change in thermal expansion is associated with a change in the magnetic ordering in the material in the vicinity of the reported Curie temperature; rationalisation of this result would benefit from *in situ* magnetic neutron diffraction measurements.

In the cubic high temperature phase, the corresponding thermal expansion coefficient is measured to be 13×10^{-6} °C^{-1}. During transformation, contraction of c_t initially ceases (at

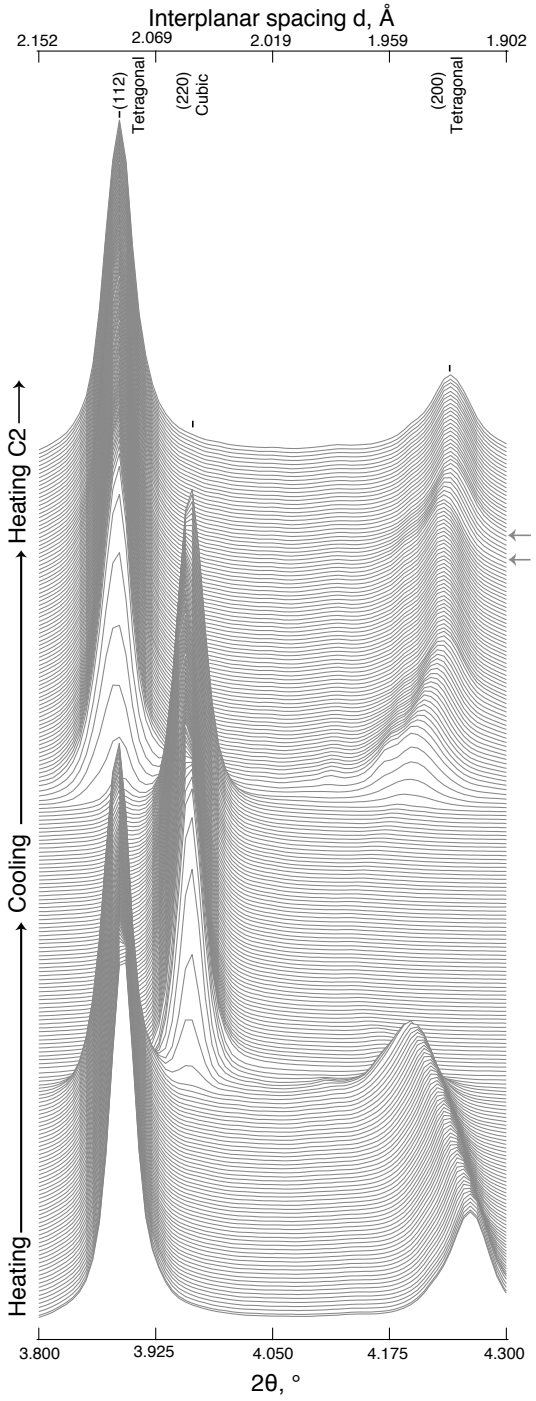

Figure 2: Evolution of (sections of the) diffraction pattern during the first thermal cycle in $Ni_{54}Mn_{25}Ga_{21}$. The e.m.f reversal regime during which a shift in martensite lattice parameters was observed is indicated by arrows on the right.

≈ 235 °C), but during the final stages of transformation it resumes; a similar behaviour in reverse is observed for a_t. During cooling, at approximately 256 °C, indicated by arrow in Figure 3, there appears to be a rather large instantaneous jump in both c_t and the austenite lattice parameter. Remarkably, this phenomenon is only observed during cooling and in case of tetragonal martensite, it is only observed in the c_t lattice parameter.

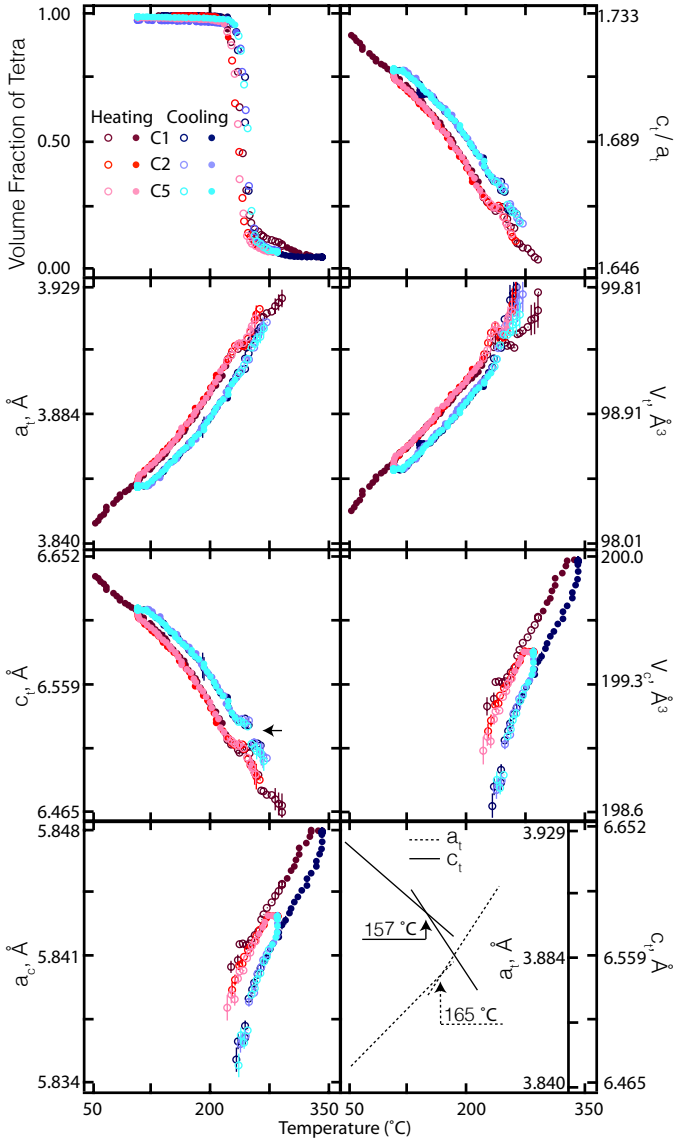

Figure 3: Tetragonal martensite and cubic austenite unit cell evolution evaluated as a function of sample temperature. Solid symbols are in thr single phase region and open symbols during transformation. 'V' is the unit cell volume and subscripts t and c signify the tetragonal and cubic phases, respectively. Cycles 1 (C1), 2 (C2) and 5 (C5) are shown.

Interestingly, a hysteresis is observed in the lattice parameters in both the cubic and tetragonal phases, not associated with the transformation itself. In the first thermal cycle (brown / dark blue) which reversed at 345°C the lattice parameters converge at that point, whereas in subsequent cycles they converge at the end point of 300°C. This is a consequence of the resistance heating method used, where the direct current applied produces an e.m.f. which, in this ferromagnetic material, results in a change in the lattice parameters. However, the Curie temperature in these alloys is widely reported to be ≈110 °C [15]. This observation therefore poses a new question such as to whether these alloys shed their ferromagnetic properties completely, or not.

The lattice parameters are shown for the first, second and

Table 1: Lattice parameters (Å) of tetragonal martensite on cooling and heating (at 125 °C for martensite and at 270 °C for austenite), where, c and h superscripts are for cooling and heating, A_s, A_f, M_s and M_f are austenite start, finish, martensite start and finish respectively.

	Cycle 1	Cycle 5
a_t^h	3.8653 ± 0.0003	3.8667 ± 0.0004
a_t^c	3.8606 ± 0.0004	3.8604 ± 0.0003
c_t^h	6.603 ± 0.001	6.600 ± 0.001
c_t^c	6.611 ± 0.001	6.612 ± 0.001
a_c^h	5.8433 ± 0.0003	5.8425 ± 0.0002
a_c^c	5.8403 ± 0.0003	5.8403 ± 0.0002
Austenite start, A_s	226	227
Austenite finish, A_f	298	258
Martensite start, M_s	267	268
Martensite finish, M_f	232	236

fifth thermal cycle applied. It is notable that, whilst the lattice parameters at a given temperature are invariant with cycling, the transformation temperatures do evolve, by ~ 8 K/cycle for the austenite finish temperature A_f.

The evolution of the ETMT actuator position, along with the ex-situ DSC data, are shown in Figure 4. For comparison, DSC data for binary NiTi and two $Ni_{50}Ti_{35}X_{15}$ (X=Hf or Zr) high temperature shape memory alloys are also shown. The DSC results reproduce the observed transformation temperatures from the diffraction measurements and show a hysteresis (A_f-M_f) of around of 22 K in cycle 5. The austenite finish temperature gradually declines on cycling, but the martensite transformation temperatures remain constant, which is unusual compared to NiTi SMAs. In addition, the ETMT actuator position, which is in effect a dilatometry measurement over the entire sample length (some of which remained cold and did not transform), is shown. The transformation on heating results in a contraction of the sample which is reversed on cooling, but there is an evolution in the end-point actuator positions with cycling that indicates expansion of the sample from cycle 2 through 5. Since this occurs for the *fcc* austenite as well as the martensite, this cannot be due to the selection of preferred crystallographic variants and therefore must be due to the accumulation of plasticity, *i.e.* interface dislocations. By reference to conventional NiTi SMAs [32, 33], this would also be the reason for the gradual decline in the austenite transformation temperatures with cycling.

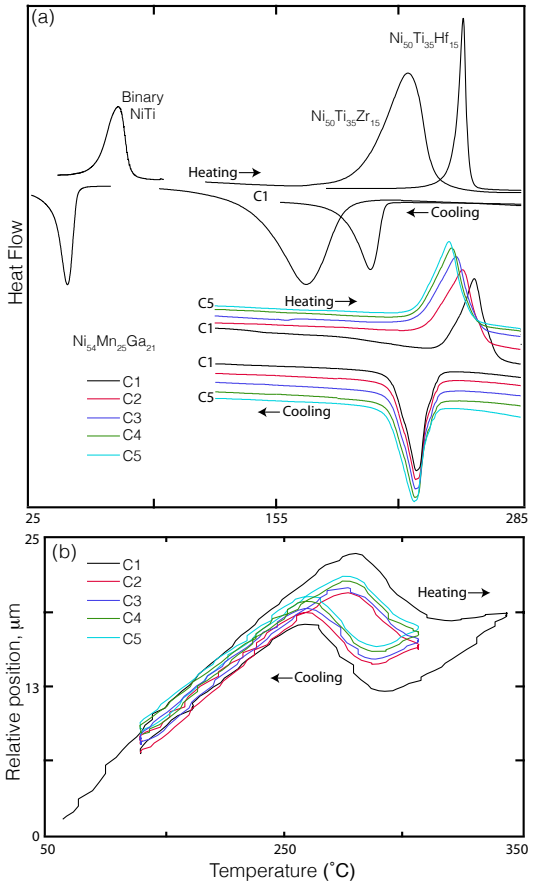

Figure 4: (a) Differential Scanning calorimeter (DSC) results obtained for five heating and five cooling cycles of as-rolled $Ni_{54}Mn_{25}Ga_{21}$ are shown, in comparison with the first cycle results for binary NiTi and as-rolled high temperature SMAs $Ni_{50}Ti_{35}Hf_{15}$ and $Ni_{50}Ti_{35}Zr_{15}$ alloys and (b) Dilation in macroscopic $Ni_{54}Mn_{25}Ga_{21}$ along the rolling direction during thermal cycling.

In summary, polycrystalline $Ni_{54}Mn_{25}Ga_{21}$ has been produced by a conventional ingot metallurgy and hot working approach. It is found to be a viable high temperature shape memory alloy material with M_f = 236 °C. The lattice parameters measured in both phases were found to be affected by the magnetic fields induced in the specimen by the applied ohmic heating method used, even above the expected Curie temperature of the alloy. Some functional fatigue was observed in the austenite transformation temperatures on heating. The thermal expansion / contraction of the tetragonal martensite a_t and c_t cell parameters were observed to accelerate above the expected Curie temperature.

Acknowledgements

The authors gratefully acknowledge funding by Rolls Royce Plc., Imperial College and the UK-India Education and Research Initiative (UKIERI). DD acknowledges funding from EPSRC under EP/H004882/1. The assistance provided by T. Buslaps is also appreciated.

[1] V. A. Chernenko, E. Cesari, V. V. Kokorin, and I. N. Vitenko, "The development of new ferromagnetic shape memory alloys in Ni-Mn-Ga system," *Scripta Metallurgica et Materialia*, vol. 33, pp. 1239–1244, 1995.

[2] D. J. Hartl and D. C. Lagoudas, "Aerospace applications of shape memory alloys," *Proceedings of the Institution of Mechanical Engineers G – Journal of Aerospace Engineering*, vol. 221, no. G4, pp. 535–552, 2007.

[3] N. T. Birch and J. R. Webster, "Gas turbine engine exhaust nozzle having a noise attenuation device driven by shape memory material actuators," US Patent US6813877B2, 2004.

[4] Y. Li, D. Zhao and J. Liu, "Giant and reversible room-temperature elastocaloric effect in a single-crystalline Ni-Fe-Ga magnetic shape memory alloy," *Scientific Reports*, vol. 6, 25500, 2016.

[5] H. Ossmer, F. Lambrecht, M. Gültig, C. Chluba, E. Quandt and M. Kohl, "Evolution of temperature profiles in TiNi films for elastocaloric cooling," *Acta Materialia*, vol. 81, pp. 9–20, 2014.

[6] S. Qian, Y. Geng, Y. Wang and T.E. Pillsbury, Y. Hada, Y. Yamaguchi, K. Fujimoto, Y. Hwang, R. Radermacher, J. Cui, Y. Yuki, K. Toyotake, and I. Takeuchl, "Elastocaloric effect in CuAlZn and CuAlMn shape memory alloys under compression", *Philosophical Transactions of the Royal Society of London A* vol. 374, 20150309, 2016.

[7] J.-h. Kim, F. Inaba, T. Fukuda, and T. Kakeshita, "Effect of magnetic field on martensitic transformation temperature in Ni–Mn–Ga ferromagnetic shape memory alloys," *Acta Materialia*, vol. 54, pp. 493–499, Jan. 2006.

[8] A. Sozinov, A. A. Likhachev, N. Lanska, and K. Ullakko, "Giant magnetic-field-induced strain in NiMnGa seven-layered martensitic phase," *Applied Physics Letters*, vol. 80, no. 10, p. 1746, 2002.

[9] M. Chmielus, X. X. Zhang, C. Witherspoon, D. C. Dunand, and P. Müllner, "Giant magnetic-field-induced strains in polycrystalline Ni–Mn–Ga foams," *Nature Materials*, vol. 8, pp. 863–866, Sept. 2009.

[10] C. A. Jenkins, R. Ramesh, M. Huth, T. Eichhorn, P. Pörsch, H. J. Elmers, and G. Jakob, "Growth and magnetic control of twinning structure in thin films of Heusler shape memory compound Ni_2MnGa," *Applied Physics Letters*, vol. 93, no. 23, p. 234101, 2008.

[11] S. Jeong, K. Inoue, S. Inoue, K. Koterazawa, M. Taya, and K. Inoue, "Effect of magnetic field on martensite transformation in a polycrystalline Ni2MnGa," *Materials Science and Engineering A*, vol. 359, pp. 253–260, Oct. 2003.

[12] S. J. Murray, M. A. Marioni, A. M. Kukla, J. Robinson, R. C. O'Handley, and S. M. Allen, "Large field induced strain in single crystalline Ni–Mn–Ga ferromagnetic shape memory alloy," *Journal of Applied Physics*, vol. 87, no. 9, p. 5774, 2000.

[13] P. J. Webster, K. R. A. Ziebeck, S. L. Town, and M. S. Peak, "Magnetic Order and Phase-Transformation in Ni_2MnGa," *Philosophical Magazine B*, vol. 49, no. 3, pp. 295–310, 1984.

[14] H. Xu, Y. Ma, and C. Jiang, "A high-temperature shape-memory alloy $Ni_{54}Mn_{25}Ga_{21}$," *Applied Physics Letters*, vol. 82, no. 19, pp. 3206–3208, 2003.

[15] N. Lanska, O. Soderberg, A. Sozinov, Y. Ge, K. Ullakko, and V.K Lindroos, "Composition and temperature dependence of the crystal structure of Ni-Mn-Ga alloys," *Journal of Applied Physics*, vol. 95, no. 12, pp. 8074–8078, 2004.

[16] V. A. Chernenko, J. Pons, C. Seguı, and E. Cesari, "Premartensitic phenomena and other phase transformations in Ni–Mn–Ga alloys studied by dynamical mechanical analysis and electron diffraction," *Acta Materialia*, vol. 50, pp. 53–60, Jan. 2002.

[17] C. Jiang, G. Feng, S. Gong, and H. Xu, "Effect of Ni excess on phase transformation temperatures of NiMnGa alloys," *Materials Science and Engineering A*, vol. 342, pp. 231–235, Feb. 2003.

[18] S. K. Wu and S. T. Yang, "Effect of composition on transformation temperatures of Ni–Mn–Ga shape memory alloys," *Materials Letters*, vol. 57, pp. 4291–4296, 2003.

[19] J. Pons, V. Chernenko, R. Santamarta, and E. Cesari, "Crystal structure of martensitic phases in Ni-Mn-Ga shape memory alloys," *Acta Materialia*, vol. 48, no. 12, pp. 3027–3038, 2000.

[20] P. J. Brown, J. Crangle, T. Kanomata, M. Matsmuoto, K. U. Neumann, B. Ouladdiaf, and K. R. A. Ziebeck, "The crystal structure and phase transitions of the magnetic shape memory compound Ni_2MnGa," *Journal of Physics – Condensed Matter*, vol. 14, no. 43, pp. 10159–10171, 2002.

[21] M. Richard, J. Feuchtwanger, D. Schlagel, T. Lograsso, S.M Allen, and R.C O'Handley, "Crystal structure and transformation behavior of Ni-Mn-Ga martensites," *Scripta Materialia*, vol. 54, no. 10, pp. 1797–1801, 2006.

[22] Y.Q Ma, C.B Jiang, G. Feng, and H.B Xu, "Thermal stability of the $Ni_{54}Mn_{25}Ga_{21}$ Heusler alloy with high temperature transformation," *Scripta Materialia*, vol. 48, no. 4, pp. 365–369, 2003.

[23] D. Y. Cong, P. Zetterstrom, Y. D. Wang, R. Delaplane, R. L. Peng, X. Zhao, and L. Zuo, "Crystal structure and phase transformation in Ni53Mn25Ga22 shape memory alloy from 20 K to 473 K," *Applied Physics Letters*, vol. 87, no. 11, 2005.

[24] J. E. Daniels and M. Drakopoulos, "High-energy X-ray diffraction using the Pixium 4700 flat-panel detector," *Journal of Synchrotron Radiation*, vol. 16, no. 4, pp. 463–468, May 2009.

[25] H. M. Rietveld, "A profile refinement method for nuclear and magnetic structures," *Journal of Applied Crystallography*, vol. 2, no. 2, pp. 65–71, June 1969.

[26] B. H. Toby, "EXPGUI, a graphical user interface for GSAS," *Journal of Applied Crystallography*, vol. 34, no. 2, pp. 210–213, 2001.

[27] A. C. Larson and R. B. Von Dreele, "GSAS: general structure analysis system," *Los Alamos National Laboratory Report LAUR 86-748*, 2004.

[28] A. P. Hammersley, S. O. Svensson, M. Hanfland, A. N. Fitch, and D. Hausermann, "Two-dimensional detector software: From real detector to idealised image or two-theta scan," *High Pressure Research*, vol. 14, no. 4-6, pp. 235–248, Jan. 1996.

[29] M. A. Azeem, and D. Dye, "In situ evaluation of the transformation behaviour of NiTi-based high temperature shape memory alloys," *Intermetallics*, vol. 46, pp. 222–230, 2014

[30] M. A. Azeem, and D. Dye, "Lattice instability during the martensitic transformation in the high temperature shape memory alloy Zr (Cu 0.5 Co 0.25 Ni 0.25)," *Journal of Alloys and Compounds*, vol. 618, pp. 469–474, 2015

[31] D. Y. Cong, Y. D. Zhang, Y. D. Wang, M. Humbert, X. Zhao, T. Watanabe, L. Zuo, and C. Esling, "Experiment and theoretical prediction of martensitic transformation crystallography in a Ni–Mn–Ga ferromagnetic shape memory alloy," *Acta Materialia*, vol. 55, no. 14, pp. 4731–4740, 2007.

[32] N.G.Jones, D. Dye. "Martensite evolution in a NiTi shape memory alloy when thermal cycling under an applied load," *Intermetallics*, vol. 19, pp. 1348–1358, 2011.

[33] I. Takeuchi, O. O. Famodu, J. C. Read, M. A. Aronova, K.-S. Chang, C. Craiciunescu, S. E.Lofland, M. Wuttig, F. C. Wellstood, L. Knauss, A. Orozco. "Identification of novel compositions of ferromagnetic shape-memory alloys using composition spreads," *Nature Materials*, vol. 2, no. 3, pp. 180–184, 2003.